paper no. 55—A-156

The American Society of Mechanical Engineers

29 WEST 39TH STREET, NEW YORK 18, NEW YORK

THE SLOTTED BLADE AXIAL-FLOW BLOWER

Dr. H. E. Sheets, Member ASME
Chief Research and Development Engineer
Electric Boat Division
General Dynamics Corporation
Groton, Conn.

Contributed by the Hydraulic Division for presentation at a joint session of the Hydraulic and Gas Turbine Power Divisions at the ASME Diamond Jubilee Annual Meeting, Chicago, Ill. - November 13-18, 1955. (Manuscript received at ASME Headquarters September 7, 1955).

Written discussion on this paper will be accepted up to January 10,1956.

(Copies will be available until October 1, 1956)

Price: 50 cents per copy
(25 cents to ASME members)

ABSTRACT

The slotted blade applies boundary-layer control to the blades of axial-flow blowers. This offers a means to design axial-flow blowers for higher efficiencies or higher pressure coefficient, or possibly a combination of both. Test data of an experimental blower are presented, indicating blower efficiencies to 94 per cent and stage efficiencies to 96 per cent with high-pressure coefficient corresponding to a maximum flow deflection of about 52 deg.

THE SLOTTED BLADE AXIAL-FLOW BLOWER

By H. E. Sheets

NOMENCLATURE

The following nomenclature is used in the paper:

c = blade chord

D = impeller tip diameter, ft

D_H = impeller hub diameter, ft

H = total head, ft

n = revelutions per sec

n_s = specific speed

Q = volume of flow, cfs

t = blade pitch

v = absolute velocity, fps

u = circumferential velocity of impeller tip, fps

w = relative velocity, fps

ϕ = flow coefficient

ψ = pressure coefficient

η = total efficiency

ρ = density of air

ν = hub ratio

Other symbols will be defined in the text.

INTRODUCTION

The slotted blade applies boundary-layer control to the blades of an axial flow blower. The subject of boundary-layer control has attracted considerable attention in respect to the isolated airfoil (1)[1] but few data exist for its application to the blades of turbomachinery. The object of boundary-layer control is to delay the transition from a laminar to a turbulent boundary-layer, thereby reducing skin friction, or to prevent boundary-layer separation, thus increasing permissible blade loading.

---

[1] Numbers in parentheses refer to the Bibliography at the end of the paper.

Boundary-layer control has been accomplished by the application of either suction or pressure to the boundary layer. One system uses an independent source of suction, or pressure, to remove or add fluid to the boundary layer; whereas another system uses slots or auxiliary airfoils, and accomplishes the same effect by using the pressure difference between the upper and lower surfaces of the airfoil for boundary-layer control. In the form of slotted flaps, boundary-layer systems are used on standard airplane wings, and a number of experimental airplanes have been flown with various types of suction and ejection systems operated from an independent pressure source.

The advantages of boundary-layer control systems for blades of compressors have been recognized (2) but experimental data have been disappointing. Tests using suction slots energized by an independent pressure source, as well as tests with slotted blades energizing the boundary-layer by flow from the lower to the upper blade surface indicate about 75 per cent efficiency, a lower efficiency than for standard blades (3). The low efficiencies are ascribed to the increased profile drag caused by the slots and to the blade arrangement which produces large secondary flows, causing, in turn, high losses. A higher pressure coefficient and higher turning angles have been achieved.

The application of boundary-layer control to the blades of turbomachinery is considerably more complex than its application to the isolated airfoil because of the added problems of secondary flow (2), of three-dimensional effects due to the twisted blades, of radial distribution of flow, and of the effects of centrifugal force and pressure distribution on the boundary layer.

An analysis of boundary-layer control applied to the blades of a blower is presented herein. The slotted-blade construction is used, producing boundary-layer control by means of the flow from the lower to the upper surface in cascades of airfoils. Variables for the geometry of the slot are analyzed, and test data are submitted for one blower, resulting in both high efficiency and pressure coefficient.

ANALYSIS

Boundary Layer

The boundary layer is the film of fluid immediately adjacent to the blades moving the fluid through the impeller. In this boundary layer viscous forces predominate, whereas outside the boundary-layer viscosity is unimportant because the velocity gradient is small. There are two types of boundary layer; namely, laminar and turbulent. In the laminar layer, the flow is smooth and without eddies. In the turbulent layer a large number of relatively small eddies exist. These eddies in the turbulent boundary layer induce transfer of momentum from the outer parts of the fluid, moving with high velocity, to the fluid from close to the surface, resulting in a velocity distribution having a higher velocity near the surface. Due to this mechanism of fluid flow, skin friction of the turbulent boundary layer is higher than for the laminar flow.

For ideal fluid flow, the flow analysis on airfoils is represented by pressure and velocity distribution as a function of airfoil chord. The boundary-layer flow at its outer limit equals the ideal flow but due to the viscous forces, the flow within the boundary-layer is more complex. In the areas of flow deceleration,

the loss of speed is greater for the particles of fluid in the boundary layer than for those in the outer flow because of the reduced kinetic energy in the boundary layer, thus limiting boundary-layer flow against adverse pressure gradients. The particles of the fluid within the boundary layer may actually reverse their motion if the rise in pressure exceeds a critical value, and then the flow is separated from the airfoil.

Turbulent boundary layers are less inclined to separation than laminar layers because of the increased interchange in momentum. If laminar-flow separation occurs, the flow may leave the surface permanently or reattach itself in the turbulent boundary layer. If turbulent-flow separation occurs, it can affect the flow through the guide vanes or the next row of blades.

Flow through airfoils displays a region of laminar flow beginning at the leading edge. Further downstream, at approximately the location of the minimum pressure, there is a transitional region in which the distribution of the mean boundary-layer velocity changes, and finally, there is a region of fully developed turbulent motion. As the fluid moves over the airfoil, the boundary layer is initially thin in the laminar-flow section, and thickens as the flow progresses along the surface and changes to a transitional and turbulent boundary layer. The extent of the laminar, transitional, and turbulent boundary layer along the airfoil is a function of the blade geometry, blade loading, Reynolds number, and turbulence in the general flow stream. In addition, irregularities on the surface may cause an earlier transition to turbulent flow. Thickness, and increase in thickness, of the boundary layer are a function of the local pressure gradients, Reynolds number, and surface conditions. If no separation occurs, the airfoil drag is primarily caused by skin friction and the value of the drag depends mainly on the relative amounts of laminar and turbulent boundary-layer flow. For further analysis of the drag, the relationship between pressure distribution and frictional intensity is of particular interest.

The total drag of the airfoils in cascade consists of form drag which is a function of the normal pressure and skin friction drag which is associated with the tangential stress acting on the surface of the airfoil or frictional intensity (4). Frictional intensity is also defined by multiplying the velocity gradient in the boundary layer at the airfoil surface with the viscosity of the air (5). Thus, frictional intensity can be determined experimentally.

Fig. 1 shows data of pressure distribution and frictional intensity both in dimensionless form by dividing their corresponding values by the value of free-stream energy $1/2\rho v^2$ for the upper surface of an airfoil. On the upper surface, frictional intensity has one maximum value near the forward section, and a second and larger maximum value a certain distance downstream on the airfoil chord. The transition from laminar to turbulent flow in the boundary layer takes place in the region between these two maxima. Usually the transitional region moves towards the forward section as the blade loading increases. Distribution of normal pressure indicates that the transitional region is situated just downstream of the point of lowest absolute pressure. The distribution of frictional intensity on the lower surface resembles that on the upper surface, but the maximum values are smaller. It appears that the frictional intensity reduces towards the trailing edge, provided that no separation of flow occurs on either the upper or lower surface. It must be remembered that the values for frictional intensity will vary just like the values for pressure distribution with airfoil parameters like camber, thickness, cascade

solidity and stagger angle and for the same airfoil it will vary with blade loading or angle of attack. Attempts to prevent the boundary layer from becoming turbulent, or separating from the body, by means of suction or blowing systems, are termed "boundary-layer control."

The National Advisory Committee of Aeronautics, NACA (6) has developed laminar-flow airfoils by designing airfoils of such a configuration as to give a slowly decreasing pressure distribution over a predetermined extension of the chord of the airfoil. The theory has been developed (7, 8) so that it can supply the shape of an airfoil to give a calculated velocity and pressure distribution, including consideration of the boundary layer in cascades (9). The laminar-flow airfoils have a laminar boundary layer over a certain extension of the chord, with sudden change in pressure gradient and transition to turbulent boundary layer. Airfoils have been designed with laminar flow to about 60 per cent of the blade-chord length. There are distinctive advantages of low drag when these airfoils are used within the range of optimum conditions for which they are designed. However, these airfoils are sensitive to proper blade loading.

Fig. 2 shows the lift and drag coefficients for one conventional and two laminar-flow airfoils. Outside the normal range of blade loading, the laminar-flow airfoil can have a higher drag coefficient than conventional airfoils.

In cascades of airfoils for blowers, there is a pressure gradient between the inlet and the exit of the blade row resulting in higher local values of deceleration and pressure increase on the airfoil, as shown in Fig. 3. In this figure, it is apparent that the pressure rise along the low-pressure side of the airfoil in cascade is considerably steeper than the equivalent rise in the case of the isolated airfoil. Cascades of blowers become considerably more sensitive in their transition from laminar to turbulent boundary layer and to separation as the pressure increase per row of blades is increased.

The Slotted Blade

The slotted blade establishes a flow from the lower to the upper side of the airfoil for the purpose of boundary-layer control. This results in a sink and boundary-layer removal on the lower side of the airfoil, and a source with ejection of fluid on the upper side of the airfoil. In order to achieve a minimum drag, a dropping pressure is desirable over the initial part of the airfoil surface upstream of the slot location, using the principle of the NACA laminar-flow airfoils. On the upper blade surface, a laminar boundary layer is maintained to a predetermined point along the blade chord where ejection of fluid occurs, resulting in addition of energy to the boundary layer and simultaneously in a pressure change. This establishes quick transition to a turbulent boundary layer.

The formation of a turbulent boundary layer at this point on the upper airfoil surface is really advantageous, because the air is thereby given more momentum to follow the rest of the airfoil surface. If the transition to a turbulent boundary layer is delayed so much that the laminar boundary layer separates, and stays separated, then the result is an increased drag coefficient. The location and amount of fluid ejection producing energy addition can be controlled, thus permitting flow without separation against the necessary steep pressure gradient.

This will permit the design of airfoils with favorable pressure distribution

and laminar flow over great portions of the chord even for highly cambered airfoils. The lower blade surface has a flow sink and removal of the boundary layer, thereby extending the range of laminar flow to approximately the trailing edge under design conditions. This reduces frictional drag by reducing frictional intensity. A pronounced reduction in drag is obtained by the reduction of the skin friction through increasing the relative extent of the laminar boundary layer on the lower airfoil surface. The slotted blade is designed to have a greater extent of laminar flow over the lower airfoil surface than over the upper surface, and the relative extent of total laminar flow is increased.

The theory of stability of the laminar boundary layer indicates that transition to turbulence may be induced by the presence of disturbances and by surface roughness. Therefore, the flow in the vicinity of the slot must be carefully analyzed and the slot be designed accordingly.

It should be noted that the characteristics of a slotted laminar-flow airfoil may show the typical narrow range of low drag followed by a higher drag outside the design range. This, in turn, requires for maximum efficiency careful analysis of the blades from hub to tip, so that at the point of maximum efficiency all airfoil sections operate within the optimum range. The entire flow problem is three-dimensional and considerable attention has to be given to secondary flows and movement of the boundary layer, requiring analysis of flow and pressure at the slot location, as well as at the trailing edge, between hub and tip. The importance of proper radial distribution of pressures has led to a change in the respective slot location and configuration. The pressure difference between the upper and lower side of the airfoil determines the amount of fluid flow through the slot and this quantity of flow and the relative pressure change at the slot are varied between hub and tip. The same type of airfoils are used, having a higher cambered profile at the hub, a lower cambered profile at the tip, and a variable degree of laminar flow due to the change in slot location.

Much greater increase in blade loading and stage-pressure ratio should be possible through the use of boundary-layer control on the rotor and stator blades. There should be no difficulty in doubling the loading obtainable without boundary-layer control. It is less easy to evaluate the effect of boundary-layer control on the efficiency of the stage in the entire blower. The profile lift-drag ratio should be increased because larger lift coefficients and corresponding flow deflections are possible. In addition, there is a decrease of profile drag, and the stage efficiency should, therefore, be higher than for conventional blades, provided the secondary blade losses are not increased. The principle should be particularly beneficial for small Reynolds numbers. Boundary-layer control offers a means to design blowers for either higher efficiencies, or higher pressure ratios, or possible, a combination of both.

DESIGN OF BLOWER

The following dimensionless coefficient (10, 11) are used for the design and presentation of the performance data:

Flow coefficient $\phi = \frac{v_m}{U} = \frac{Q}{D^3 n} \quad \frac{4}{\pi^2 (1-\nu^2)}$

Pressure coefficient $\psi = \frac{2gH}{U^2} = \frac{2gH}{D^2 n^2 \pi^2}$

Specific speed $n_s = \frac{n Q^{1/2}}{g^{3/4} H^{3/4}}$

Hub ratio $\nu = \frac{D_H}{D}$

An experimental blower was designed to meet the following specifications:

Q = 40 cfs	ϕ = 0.580	ν = 0.744
p = 2.80 in. water	ψ = 0.900	
n = 1750 rpm	n_s = 0.262	

This blower has a pressure coefficient which is beyond the range of ordinary blading requiring a deflection of the air of 52 deg at the hub of the rotor and stator. Therefore, a design with slotted blades was undertaken. A casing diameter of 15.5 in. and a hub diameter of 11.5 in. were selected. The Reynolds number is R_c = 252,000 based on the impeller-blade chord and R_b = 142,000 based on the inlet area of the flow passage.

It was desirable to extend the range of capacity and pressure for this blower and still maintain the same physical configuration. Therefore, the blower was designed to permit adjustment of the angle of incidence of the impeller blades, and to increase the speed to 3500 rpm by exchanging motors. The motor is supported within a cylindrical housing of the same diameter as the hub of the blower as shown in Fig. 4. Therefore, the selection of the hub diameter was limited by the physical size of the motors which drive the blower. A provision was made for an axial diffuser although for the standard unit no diffuser will be used due to the limitation in axial length.

The blower was designed according to the free-vortex type of flow, which requires a larger amount of twist of the blading between hub and tip, and therefore is probably more critical with regard to disturbance by secondary flow. Fig. 5 shows the vector diagrams for the experimental unit, revealing a requirement of a deflection of 22.1 deg at the tip and 52 deg at the hub for the impeller. For the stator, the deflection varies from 43.6 deg at the tip to 52 deg at the hub. It should be noted that the vector diagram at the hub is a symmetrical diagram. The design of the blade is shown in Fig. 6. The combined blade consists of two individual airfoil-type blades, so positioned relative to each other, that the larger front blade and the smaller rear blade are arranged in such a configuration that a slot is formed between the trailing edge of the front blade and the leading part of the rear blade. The combined airfoil is designed to give a nearly constant pressure distribution over about half of the blade chord on the upper surface at the design point.

The design of the blower permits variation of the blade angle of incidence to four positions. In addition to the design angle of incidence, designated as 0 deg, the combined blade can be turned to incidences of -10, +10, and +20 deg from the design condition. In addition, the blades were designed to permit the angle of deflection between the chord of front and rear blades to be varied $\pm$ 5 deg from its mean value. This type of variation results in a considerable modification of the slot geometry; and, correspondingly, the amount of flow through the slot is changed. It should be noted that the free-vortex type of flow can be expected only for the design condition designated as 0 deg. For all other conditions, the blower will operate under slightly different flow conditions. Pressure and secondary flow have been analyzed for the above blade modifications. The experimental unit was designed for easy exchange of blades and a separate set of blades was manufactured for each of the above blade modifications.

The guide vanes for this blower were designed both as solid vanes and slotted vanes. In the case of the slotted guide vanes, a configuration equivalent to the blade at the root of the impeller was selected. This was possible because the blower was designed to have a symmetrical vector diagram at the root. The design of the blower permits for the slotted blade the use of the same airfoil in the stator by selecting the stator solidity and its variation from root to tip to give the required deflection from hub to tip. A higher value of solidity was used for the solid guide vanes in order to get the required flow deflection in the stator.

The geometry and the configuration of the slot presented a complex problem, introducing many new variables into the blade design. Table 1 and Fig. 6 show the detailed data relating to the slot configuration. The cascade of airfoils is defined by the blade solidity c/t and the impeller blade stagger angle β. Solidity varies from about 1.0 at the tip to 1.38 at the hub. The combined blade is characterized by the magnitude of the camber angle θ, and the physical location of the maximum of the mean camber line along the chord designated by the dimensionless values for the abscissa h_x/c and the ordinate h_y/c. For the selected configuration, the maximum camber is located near the rear part of the mean camber line of the forward airfoil. The slotted blade is further defined by the deflection angle δ between the chords of forward and rear airfoil. This deflection angle δ varies from 21.5 deg at the tip to 37.8 deg at the hub for the standard conditions. The location of the slot on the lower airfoil surface, representing the flow sink, is defined by the distance m_x. Term m represents the width of the slot inlet, and s represents the width at the slot exit. Term o represents the distance of the slot overlap between the forward and rear airfoils. On the upper side of the blade, fluid is ejected at the location s_x for the purpose of energizing the boundary layer to avoid separation. In this analysis, the slot locations s_x and m_x, as well as the slot dimensions s and o, are all divided by the combined chord length c, and the values are presented in Table 1, together with the ratio of slot exit to inlet s/m for the design condition as well as for the modification in deflection of the rear airfoil chord. It should be pointed out that the location of the flow sink m_x/c on the lower side of the airfoil varies and moves farther forward for the higher cambered airfoil.

The same is true for the location of flow ejection s_x/c on the upper side of the combined airfoil. In addition, the amount of overlap is increased with the higher camber for the airfoil required at the root of the blades. In this particular application, the slot opening remains about constant. The larger pressure difference for the higher cambered airfoil will result in a larger amount of flow through the slot if both the slot opening and overlap remain the same. The angle γ,

of the lower surface trailing edge of the forward airfoil and the angle τ_2 of the forward part of the upper surface of the rear airfoil at the slot exit have to be carefully selected to permit the flow moving through the slot to properly energize the boundary layer of the combined profile without causing undue drag. The angles τ_1, and τ_3, together with the angle τ_m of the mean direction of flow at the slot exit, are presented in Table 1. All angles τ are measured with regard to the direction of the chord line of the forward airfoil.

There are many variables in this blade configuration which can be modified without substantially changing the concept of the slotted blade. Time did not permit analysis of all the possible modifications, and thus the selected configuration may not represent the optimum solution of the problem.

TEST DATA

The tests with the experimental blower were made over a wide range of pressures and capacities and according to the ASME, Navy, and ASHVE test codes. The test setup is shown in Fig. 4. The standard blower extends from the intake A to the blower exit C, and is tested, by measuring total pressure, static pressure, and dynamic pressure at the specified location E. Owing to the large hub-tip ratio, there is a sudden change in flow area and a loss in energy between the end of the blower at location C and the instrumentation. Therefore, additional tests were made with a diffuser attached to the blower, to analyze pressure recovery. For the tests with diffuser, the blower extends from the inlet A to the diffuser exit at G. The tests with the diffuser meet all code requirements except that the pitot tube location is now $7\frac{1}{2}$ diameters downstream of the end of the blower, now located at G, and this is taken into consideration by allowing duct friction only from the location of the pitot tube at E to the diffuser exit at G. In addition, a flow survey was made near the guide-vane exit, location C, to determine the stage efficiency of the blower. For this purpose a small pitot tube and a special yaw tube, shown in Fig. 7 were used. The energy input of the blower was determined by two wattmeters, while operating the motor with controlled voltage. The efficiency of the electric motors was determined by two independent brake tests which agreed with each other to within less than 1 per cent of accuracy.

Fig. 8 shows the performance of the blower without diffuser, with both slotted impeller and slotted guide vanes. The performance of the blower is presented in terms of dimensionless coefficients ψ over ϕ with the efficiency η as independent variable over a range of impeller-blade incidence from -10 to +20 deg. The test data indicate that the blower meets the required performance and excellent efficiencies are demonstrated, particularly for the 0 and -10 deg blade incidence.

Fig. 9 shows the efficiency of the blower without diffuser as function of the flow coefficient ϕ. Fig. 10 shows the performance of the blower with the diffuser. A significant increase in both pressure coefficient and efficiency is shown, particularly for the blade incidences +10 and +20 deg covering the range of large flow. Fig. 11 shows the efficiency of the blower with diffuser as function of the flow coefficient ϕ. It will be noted that the blower has a maximum efficiency of 91 and 94 per cent for the impeller-blade incidences of 0 and -10 deg, respectively. It is to be expected that the efficiency of this blower will be lower when the incidence of the impeller blades is turned to the +20 deg position and no adjustment of the guide vanes is made.

Fig. 12 shows the performance for solid versus slotted guide vanes and diffuser effect of the blower in terms of pressure coefficient ψ and efficiency η over the flow coefficient ϕ for the 0 deg blade incidence. As expected the pressure coefficient and efficiency improve by adding the diffuser and replacing solid with slotted guide vanes.

The stage efficiency of the blower near the point of maximum efficiency was measured at location C for slotted guide vanes with a small pitot and yaw tube. This survey of total pressure, static pressure, velocity pressure, and flow angle was made in both the radial and circumferential direction, and the values were integrated in both directions. An efficiency of about 96 per cent is shown in Fig. 12 at A. The stage efficiency also was determined from the test without diffuser by calculating the energy losses resulting from the sudden expansion of flow, and is indicated at B with a maximum efficiency of about 96 per cent.

Fig. 13 shows near the design point the axial-velocity distribution from hub to tip downstream of the guide vanes, indicating a slightly larger velocity at the hub and good agreement with the calculated data. Fig. 14 shows the integrated values of velocity in the circumferential direction. The measured values of flow deflection with the yaw tube as shown in Fig. 15 indicate nearly axial flow in the vicinity of the design point. Fig. 16 shows the blower performance as it is affected by changing the chord of the rear airfoil ± 5 deg with respect to the forward airfoil chord, resulting in a change of slot geometry, total blade camber, and type of flow. It is noted that the -5 deg position results in a maximum blower efficiency of 94 per cent.

Fig. 17 shows the conventional performance of the blower, according to the ASME Test Code, without diffuser for the 0 deg blade setting. Horsepower, static and total pressure in inches of water, as well as total and static efficiency, are plotted as ordinates over volume in cfm as abscissa. It should be noted that the values of both static and total pressure are considerably reduced in the region of flow below maximum pressure.

Fig. 18 shows the performance of the blower without diffuser for the -10 deg blade setting. The power curve in both Fig. 17 and Fig. 18 is characterized by low values in the region of low flow and highest values just beyond and close to the point of maximum blower efficiency.

CONCLUSIONS

An analysis has been made for the application of boundary-layer control to the blades of axial-flow blowers. The design of the slotted blade extends laminar flow over a larger portion of the blade chord and simultaneously permits large flow deflections. Blowers with slotted blades offer thus the possibility to design for higher efficiency or higher pressure ratio, or possibly a combination of both. The slotted blade permits a considerable increase in pressure coefficient or corresponding operation at lower tip speed for a given pressure increase. Design data for the slot geometry are discussed. Test data of an experimental blower are presented demonstrating efficiencies to 94 per cent with flow deflection of about 52 deg at the hub. The effect of solid or slotted guide vanes and the diffuser on blower performance is shown. A variation in slot geometry is tested. The blower has a maximum stage efficiency of about 96 per cent.

ACKNOWLEDGMENT

The author wishes to thank the Electric Boat Division, General Dynamics Corporation, Groton, Conn., for permission to publish this paper. The author is indebted to members of the Research and Development of the Electric Boat Division for the execution of all tests and the calculation of all test data.

BIBLIOGRAPHY

1 "Low-Drag and Suction Airfoils," by Sidney Goldstein, Journal of Aeronautical Sciences, vol. 15, April, 1948.

2 "Possible Application of Blade Boundary-Layer Control to Improvement of Design and Off-Design Performance of Axial-Flow Turbomachines," by J. T. Sinnette, Jr. and G. R. Costello, NACA TN 2371, May, 1951.

3 "Axial Compressors," by B. Eckert and F. Weinig, M.O.S. (A) Volkenrode, April, 1946, NACA Translation, Reports and Translation No. 353, February, 1947.

4 "Aerodynamic Theory," by W. F. Durand, Editor-in-Chief, Julius Springer, Berlin, Germany, 1935, vol. 3, Division G, "The Mechanics of Viscous Fluids."

5 "Modern Developments in Fluid Dynamics," by S. Goldstein, The Clarendon Press, Oxford, England, 1938.

6 "Summary of Airfoil Data," by I. H. Abbott, A.E. von Doenhoff, and L. S. Stivers, Jr., NACA Report No. 824, 1945.

7 "Method of Designing Cascade Blades with Prescribed Velocity Distributions in Compressible Potential Flows," by G. R. Costello, NACA Report 978, 1950.

8 "Detailed Computational Procedure for Design of Cascade Blades with Prescribed Velocity Distributions in Compressible Potential Flows," by G. R. Costello, R. L. Cummings, and J. T. Sinnette, NACA TR 2281, 1951.

9 "Problems and Results of Investigations on Cascade Flow," by Hermann Schlichting, Journal of the Aeronautical Sciences, vol. 21, March, 1954.

10 "The Theory and Performance of Axial-Flow Fans," by Kurt Keller, McGraw-Hill Book Company, Inc., New York, N.Y., 1937.

11 "Nondimensional Compressor Performance for a Range of Mach Numbers and Molecular Weights," by H. E. Sheets, Trans. ASME, vol. 74, 1952, pp. 93-102.

The Slotted Blade Axial Flow Blower

Captions for Illustrations

Fig. 1 Frictional intensity and pressure on the upper surface versus airfoil chord

Fig. 2 Drag versus lift coefficient

Fig. 3 Pressure distribution of airfoils

Fig. 4 Test arrangement

Fig. 5 Velocity-vector diagram

Fig. 6 Slotted blade

Fig. 7 Yaw tube

Fig. 8 Nondimensional performance without diffuser

Fig. 9 Efficiency without diffuser

Fig. 10 Nondimensional performance with diffuser

Fig. 11 Efficiency with diffuser

Fig. 12 Effects of component modification on performance

Fig. 13 Axial velocity versus blade height

Fig. 14 Integrated axial velocity in circumferential direction

Fig. 15 Yaw-tube measurements

Fig. 16 Nondimensional performance - rear blade variations

Fig. 17 Blower performance without diffuser

Fig. 18 Blower performance without diffuser

TABLE 1 AIRFOIL AND SLOT CONFIGURATION

		c/t	β	δ	Θ	h_x/c	h_y/c	m_x/c	s_x/c	s/c	o/c	s/m	τ_1	τ_3	τ_m
	-5°	1.034	44.08	16.09	49.50	0.559	0.100	0.615	0.641	0.0255	0.0269	0.639	14.6	-5.7	-1.25
TIP	0°	1.030	45.50	21.50	53.25	0.575	0.114	0.617	0.641	0.0196	0.0250	0.628	14.6	-1.4	5.2
	+5°	1.025	46.75	24.75	57.50	0.587	0.129	0.621	0.641	0.0137	0.0197	0.578	14.6	3.6	12.7
	-5°	1.186	58.83	23.42	66.25	0.556	0.136	0.604	0.634	0.0258	0.0298	0.632	18.9	3.75	15.1
MEAN	0°	1.178	55.00	30.02	71.00	0.568	0.151	0.606	0.634	0.0200	0.0280	0.606	18.9	7.8	21.1
	+5°	1.168	56.83	34.83	75.75	0.581	0.168	0.610	0.634	0.0131	0.0228	0.560	18.9	12.2	27.75
	-5°	1.405	68.00	33.25	83.75	0.556	0.176	0.592	0.618	0.0284	0.0266	0.616	22.4	5.8	19.9
ROOT	0°	1.385	69.75	37.83	89.00	0.564	0.193	0.595	0.625	0.0200	0.0300	0.555	22.4	9.25	25.1
	+5°	1.367	71.75	42.25	92.50	0.576	0.210	0.601	0.627	0.0112	0.0264	0.454	22.4	13.2	31.0

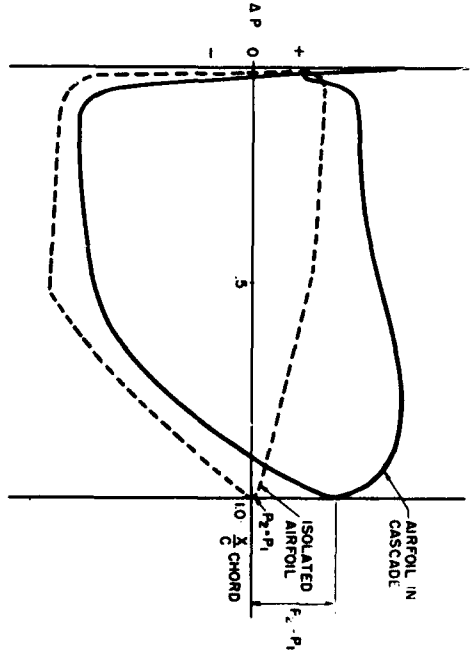

FIG. 3

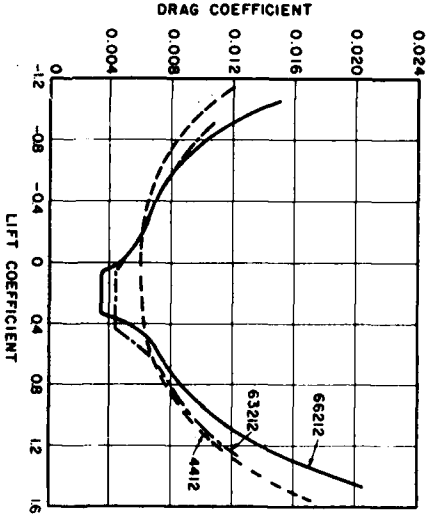

FIG. 2

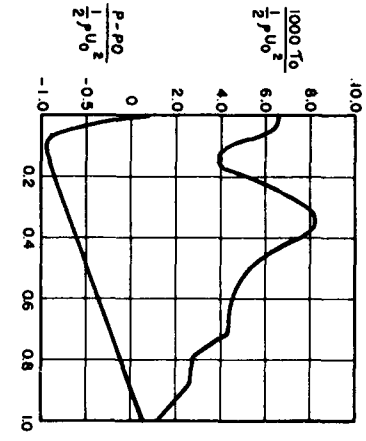

FIG. 1

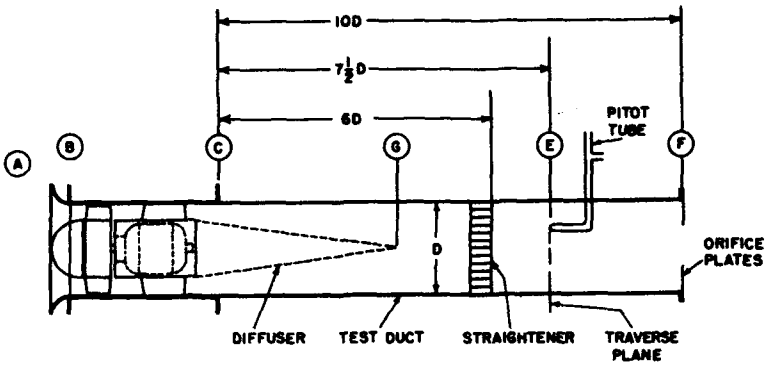

FIG.4

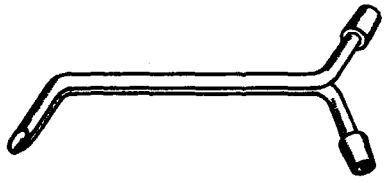

FIG.7

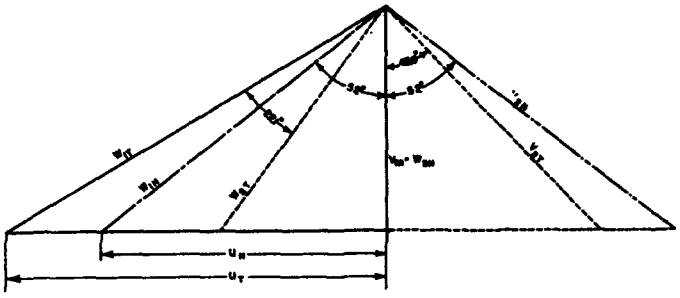

FIG.5

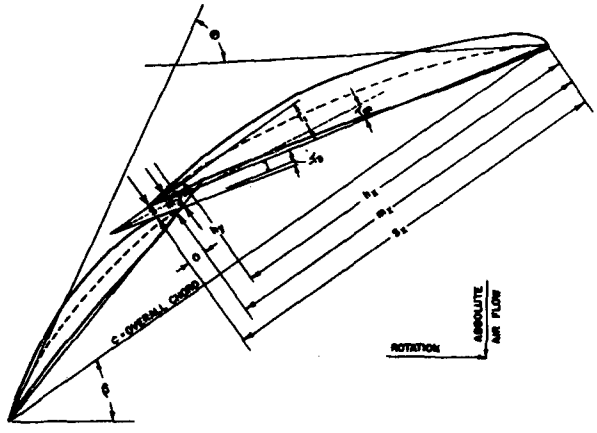

FIG.6

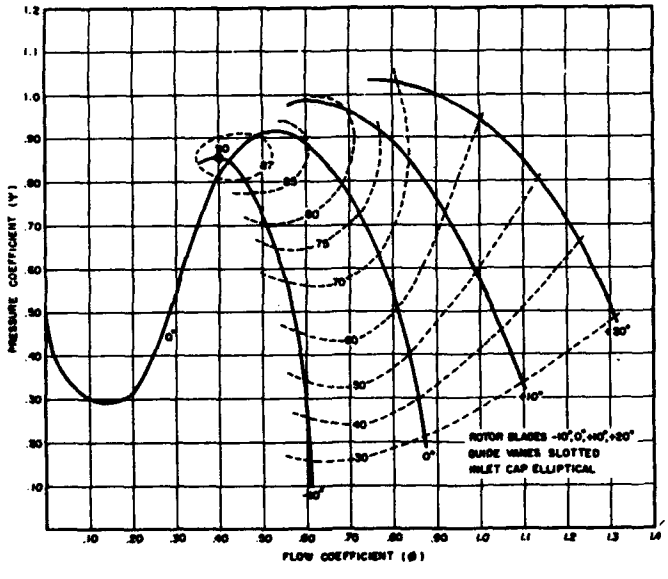

FIG.8

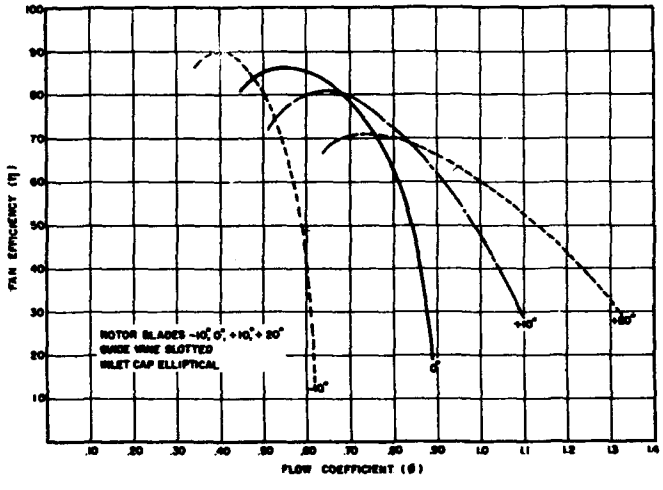

FIG.9

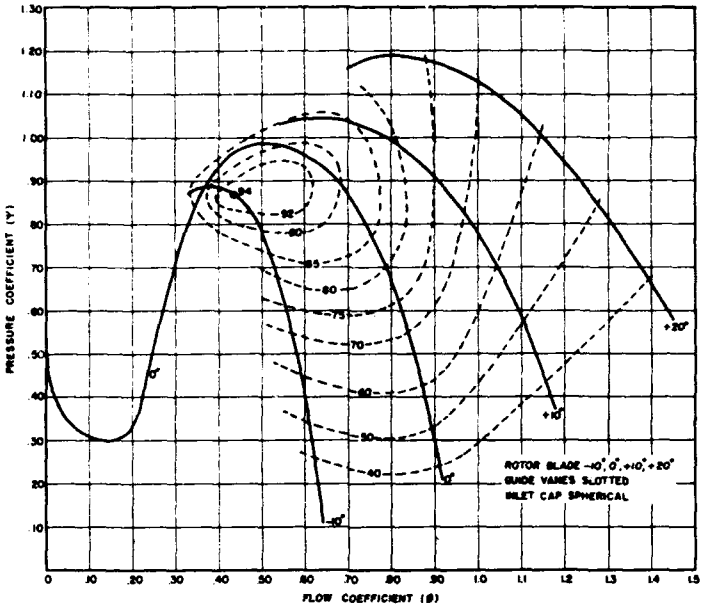

FIG.10

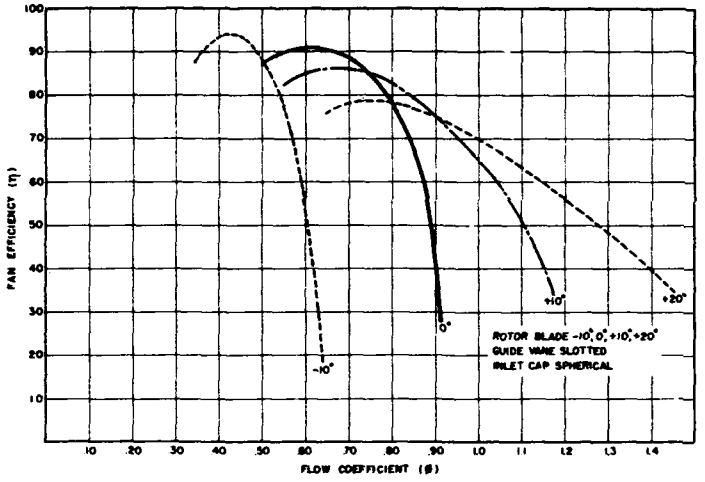

FIG.11

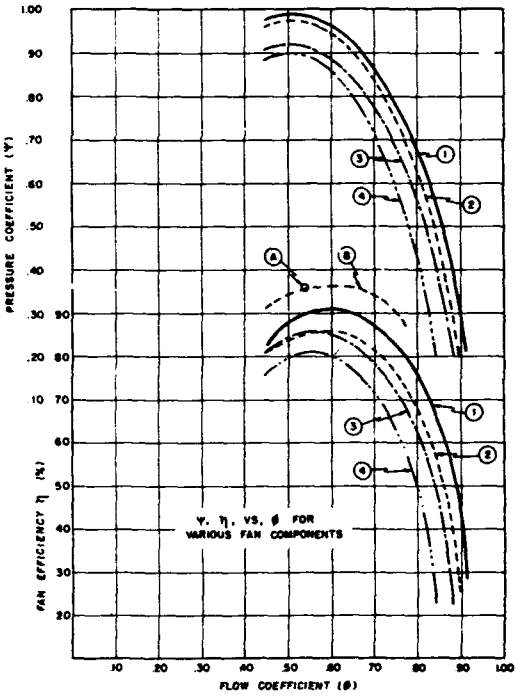

(1) Rotor 0°, Slotted Vane, Diffuser, Spherical Cap.
(2) Rotor 0°, Solid Vane, Diffuser, Spherical Cap.
(3) Rotor 0°, Slotted Vane, _____, Elliptical Cap.
(4) Rotor 0°, Solid Vane, _____, Elliptical Cap.
(A) Rotor 0°, Slotted Vane, Diffuser, Spherical Cap, Stage Efficiency Measured.
(B) Rotor 0°, Slotted Vane, Diffuser, Spherical Cap, Stage Efficiency Calculated.

FIG.12

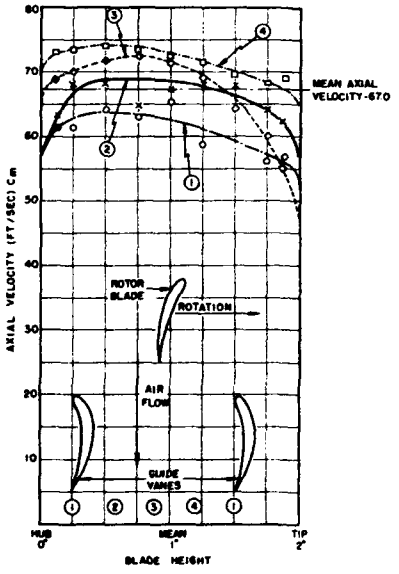

FIG.13

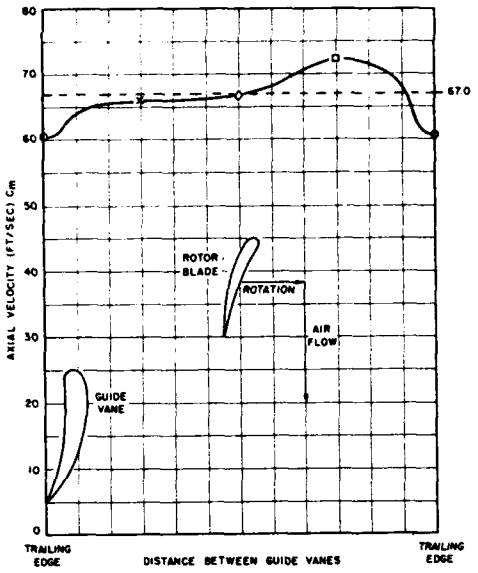

FIG.14

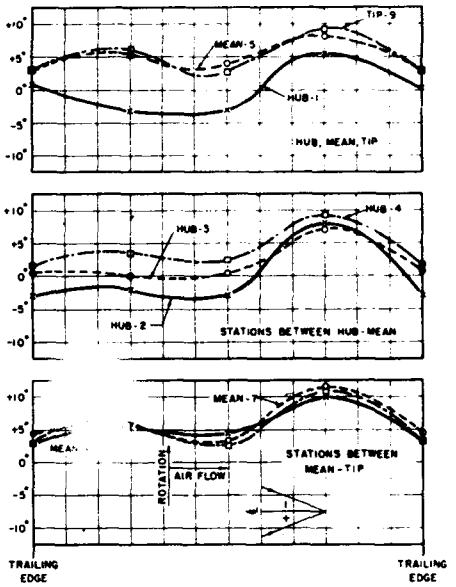

FIG.15

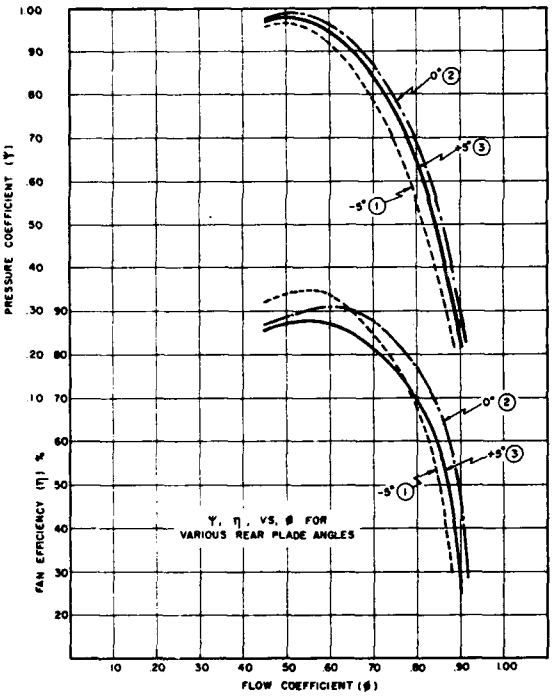

(1) Rear Blade -5° Slotted Vanes, Diffuser, Spherical Cap.
(2) Rear Blade 0° Slotted Vanes, Diffuser, Spherical Cap.
(3) Rear Blade +5° Slotted Vanes, Diffuser, Spherical Cap.

FIG.16

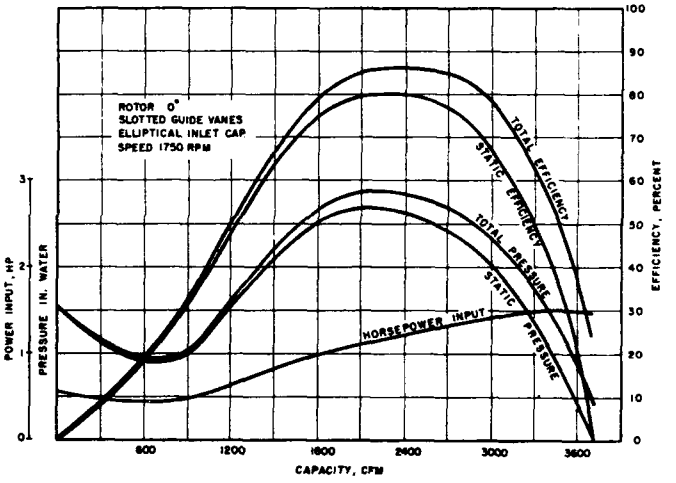

FIG.17

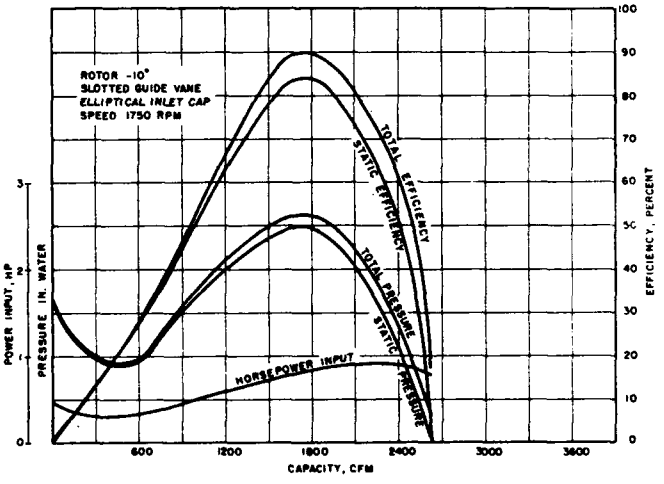

FIG.18